Published in final edited form as:
Nat Ecol Evol. 2019 October ; 3(10): 1409–1414. doi:10.1038/s41559-019-0990-3.

The earliest evidence for mechanically delivered projectile weapons in Europe

Katsuhiro Sano[1,*], **Simona Arrighi**[2,3], **Chiaramaria Stani**[4], **Daniele Aureli**[3,5], **Francesco Boschin**[3], **Ivana Fiore**[6], **Vincenzo Spagnolo**[3], **Stefano Ricci**[3], **Jacopo Crezzini**[3], **Paolo Boscato**[3], **Monica Gala**[6], **Antonio Tagliacozzo**[6], **Giovanni Birarda**[4], **Lisa Vaccari**[4], **Annamaria Ronchitelli**[3], **Adriana Moroni**[3], **Stefano Benazzi**[2,7]

[1]Center for Northeast Asian Studies, Tohoku University, Sendai, Japan

[2]Department of Cultural Heritage, University of Bologna, Ravenna, Italy

[3]Dipartimento di Scienze Fisiche, della Terra e dell'Ambiente, UR Preistoria e Antropologia, Università degli Studi di Siena, Siena, Italy

[4]Elettra-Sincrotrone Trieste S.C.p.A., Trieste, Italy

[5]UMR 7041, équipe AnTET, Université de Paris X-Nanterre, Paris, France

[6]Bioarchaeological Service, Museo delle Civiltà. Museo Preistorico Etnografico "Luigi Pigorini", Rome, Italy

[7]Department of Human Evolution, Max Planck Institute for Evolutionary Anthropology, Leipzig, Germany

Abstract

Microscopic analysis of backed lithic pieces from the Uluzzian technocomplex (45-40kya) at the Grotta del Cavallo (southern Italy) reveals their use as mechanically delivered projectile weapons, attributed to Anatomically Modern Humans. Use-wear and residue analysis indicates the lithics were hunting armatures hafted with complex adhesives, while experimental and ethnographic comparison supports their use as projectiles. The use of projectiles conferred a hunting strategy with a higher impact energy and a potential subsistence advantage over other populations and species.

[*]**Correspondence and requests for materials and data** should be addressed to K.S.

Data availability

The authors declare that data supporting the findings of this study are available within the paper and its supplementary information.

Author Contributions

A.M. and K.S. conceived and organized the project; S.B. obtained funding and directed the project; K.S. undertook the use-wear analysis with S.A as well as the morphometric analysis; C.S., G.B., and L.V. performed the residue analysis; D.A. conducted the experiment for producing Uluzzian backed pieces; I.F., M.G., and A.T. provided data about the exploitation of feathers; F.B., J.C., and P.B. presented the results of the zooarchaeological analysis; K.S., C.S., V.S., S.R., and I.F made figures and illustrations; D.A., F.B., A.R., and A.M. provided permits for the analysis of the archaeological samples and expertise on site sequences and materials; and K.S., C.S., A.R., A.M., and S.B. wrote the manuscript with contributions from all co-authors.

Competing interests The authors declare no competing interests.

Europe PMC Funders Author Manuscripts

Introduction

The Uluzzian was traditionally recognized as a one of the Middle to Upper Paleolithic transitional cultures recognized in southern Europe (i.e., Italy and Greece), but has been recently re-defined as an Early Upper Palaeolithic culture[1]. Grotta del Cavallo (Fig. 1), excavated by A. Palma di Cesnola and P. Gambassini between 1963 and 1986, is a pivotal site for the Uluzzian because its stratigraphic sequence includes three main Uluzzian layers, namely from EIII (archaic Uluzzian), EII-I (evolved Uluzzian), to D (final Uluzzian)[1] (Supplementary Fig. 1), sandwiched by the tephra Y-6 at 45.5 ± 1.0 ka[2] and Y-5 (Campanian Ignimbrite) at 39.85 ± 0.14 ka[2,3].

The Uluzzian technocomplex exhibits features that are typically associated with modern human assemblages (Supplementary Information 2) and characterized by the presence of ornaments, bone implements[4], coloring substances[5], and crescent-shaped backed pieces made on small blades or bladelets[1]. These crescent-shaped backed pieces (also referred to as lunates or segments) are a hallmark[1,6] of the Uluzzian and exhibit no techno-morphological link to the Mousterian or Initial Upper Paleolithic assemblages in Europe prior to the Uluzzian. Similar backed pieces on bladelets have been observed in East Africa, although there is no archaeological evidence indicating a route from East Africa into Europe[5]. To better understand the differences between the Uluzzian and earlier lithic traditions, as well as the significance of the emergence of this new technocomplex in Europe, it is crucial to identify the function of the backed pieces.

The excavations of Grotta del Cavallo unearthed numerous backed pieces[6], and we undertook a systematic use-wear analysis of a total of 146 of them from the three Uluzzian layers. This analysis indicates that the major function of the Uluzzian backed pieces was hunting (Supplementary Table 1). Only seven pieces were used for functions other than hunting (cutting and scraping). Out of the 146 backed pieces, 26 show 55 diagnostic impact fractures (DIFs), which form only when stone tips hit an animal target (Fig. 2). Among them, 9 backed pieces (34.6%) bear DIFs only at a single portion, while 17 (65.4 %) yield multiple DIF types (Supplementary Table 2, Supplementary Fig. 2). As several projectile trials resulted in no fractures or only non-diagnostic ones[7,8], the number of DIFs indicates the minimum number of specimens used as hunting weapons. Six pieces showed microscopic linear impact traces (MLITs) as well (Fig. 2a, f), proving that they were securely used as hunting armatures.

Most of the Uluzzian backed pieces showed residues on the back, suggesting that this portion was covered by a type of adhesive (Supplementary Fig. 3). We therefore performed Fourier-transform infrared (FTIR) spectromicroscopy on these pieces to characterize the chemical nature of the residues and identified them as a mixture of both organic and inorganic components, mainly ochre, a plant/tree gum and beeswax. The main absorption bands attributed to the organic fraction are highlighted by grey shaded area (Fig. 2o) (see Methods for more details). In addition, FTIR spectroscopy analyses of several red deposit and soil samples recovered from Grotta del Cavallo enabled us to rule out the presence of organic contaminants from the burial environment and to confirm the presence of ochre as a mixture of silicate and iron oxides by correlative Scanning Electron Microscopy/Energy

Dispersive X-ray (SEM/EDX) measurements (see Supplementary Figs. 4, 5). Together, the obtained results allowed us to postulate that the three adhesive components had been intentionally mixed, as known in the middle Upper Paleolithic context[9].

To reconstruct the hafting modes of Uluzzian backed pieces, the frequency of the DIF types (Supplementary Fig. 2) was compared to those obtained by projectile experiments with backed piece replicas[10,11]. The projectile experiments indicated that hafting as barbs resulted less often in multiple DIFs, compared with when the pieces were hafted as tips. Among the multiple DIF types, the type a2m (flute-like, burin-like, or transverse fractures from bidirectional ends) was dominant in the Cavallo backed pieces (Fig. 2b–2f) and occurred only in experiments with tip hafting (straight/oblique hafting). We do not rule out the possibility that some Uluzzian backed pieces were hafted as barbs because of the relatively high frequency of type a2 (burin-like fracture from steep angle) (Fig. 2a), which occurred in barb hafting as well. However, the frequency of the DIF types suggests that several Uluzzian backed pieces were attached on the tip of a wooden shaft.

Uluzzian backed pieces are notably small: complete or almost complete backed pieces with DIFs measured an average of 27.1 mm in length, 10.5 mm in width, and 4.6 mm in thickness (Supplementary Fig. 6a). The tip cross-sectional area (TCSA) and tip cross-sectional perimeter (TCSP) of Cavallo backed pieces with DIFs were compared to those of ethnographic North American dart tips and arrowheads[12,13]. The boxplots of the TCSA and TCSP of the Uluzzian backed pieces with DIFs fell within the range of those of North American ethnographic arrowheads, while they concentrated on a smaller range (Supplementary Fig. 6b, c). The Uluzzian backed pieces are significantly smaller than the ethnographic dart tips in terms of TCSA and TCSP (TCSA: $t = -9.414$, $p < 0.05$; TCSP: $t = -13.650$, $p < 0.05$), and even smaller than the ethnographic arrowheads (TCSA: $t = -2.773$, $p < 0.05$; TCSP: $t = -5.709$, $p < 0.05$). The extremely small dimensions of the Uluzzian backed pieces suggest that they are suitable for neither thrusting nor throwing spear tips (Supplementary Fig. 7a, b).

Despite the small size, the DIFs found on Cavallo backed pieces are relatively large: the largest DIF measures 24.7 mm in length and nine DIFs are larger than 10 mm. Several pieces show a significant reduction in the body due to impact damage (Fig. 2b, d, e). Even if specimens retain almost their original length, they often bear elongated DIFs along the side or on the surface. Remarkably, the lengths of several elongated DIFs (flute- and burin-like fractures) exceed 20% of the entire length of the backed pieces and four DIFs have a length greater than half the entire length of the specimens (Supplementary Table 3). The relatively large dimensions of DIFs suggest that the backed pieces were delivered at high impact velocities.

As at least several Uluzzian backed pieces were hafted on the tip of a wooden shaft, the small dimensions of the backed pieces must reflect the small diameter of the shaft. If a thinner shaft is used, the total size of the hunting weapon is smaller. Therefore, large DIFs, as well as multiple DIF types, occur only when the impact velocity is as high, as that upon mechanical delivery, including that for spearthrower- or bow-shooting[8]. Although the TCSA and TCSP values indicate that the projectile capability of the Uluzzian backed pieces is

closer to that of the North American arrowheads than to that of dart tips, we do not have sufficient information to discriminate between them. Nonetheless, because of the assumed velocity based on the DIF pattern, it is more plausible that the Uluzzian backed pieces were projected using either a spearthrower or a bow.

A higher impact energy, however, requires more stable hafting, since otherwise, stone tips can easily be displaced. A complex mixture, characterized by the addition of beeswax and ochre, increases the mechanical properties of the adhesive, making it less brittle[14]. The use of the complex adhesive demonstrated by FTIR spectroscopy in this study suggests that hunters at Grotta del Cavallo used advanced hafting technology for projectiles with higher impact velocity.

While the mechanical projectile system enables a higher impact velocity and long-range shooting, fletching to the base of the shaft is necessary to propel armatures in a straight trajectory. The discovery of cut marks due to the removal of feathers from bird remains at the Uluzzian site of Castelcivita (southern Italy) (Supplementary Information 3) indicates that the fletching technology was also practiced by the Uluzzian people.

The multiple findings, such as use-wear patterns, significant smallness of the Uluzzian backed pieces, and complex adhesives, presented by Grotta del Cavallo dated between 45 ka and 40 ka constitute the earliest evidence for the use of mechanically delivered projectile weapons in Europe, which is more than 20,000 years earlier than previously thought. In Europe, the earliest direct evidence for spearthrowers was found from a Solutrean layer at Combe Saunière, France, dated between ~23 ka and ~20 ka[15], and for bows-and-arrows preserved in peat bogs at an Ahrensburgian site of Stellmoor, Germany, at 12.9–11.7 ka[16]. Taking into account that most of the ethnographic spearthrowers are made of perishable materials, such as wood[17], it is no wonder that we have only much younger archaeological remains of spearthrowers and bows-and-arrows.

Neanderthals used wooden spears[18] and might also have used stone-tipped ones[19]. Their possible stone spear tips, including Levallois and Mousterian points, are overall much larger than the Upper Paleolithic points[20]. Although micro-points recovered from layer E (Neronian) of Grotte Madrin, France that might be ~5,000 years older than the Uluzzian appearance in Europe are significantly small[21,22], a systematic use-wear analysis is required to detect their function. Based on the current state of studies on Neanderthal hunting[23], their spears were basically hand delivered (thrusting or throwing), but not mechanically projected. Conversely, evidence from Africa suggests that modern humans innovated mechanically delivered projectile weapons before they expanded out of Africa[20,24]. Although the association between the Uluzzian technocomplex and modern humans has been challenged[25], the information currently available from Grotta del Cavallo link the Uluzzian to modern humans. In particular, the two deciduous teeth retrieved from the Uluzzian layers of Grotta del Cavallo were attributed to modern humans[26], and their association with the Uluzzian materials has been recently confirmed by excavation field notes[1] (Supplementary Information 1) and the stratigraphic sequence[2].

If further studies confirm the attribution of the Uluzzian to modern humans, we suggest that modern humans equipped themselves with new projectile technology when they migrated into Europe at around 45 ka. Zooarchaeological data on faunal remains from Grotta del Cavallo indicate more intensive exploitation of young horses at the Uluzzian levels than that seen at the late Mousterian (Supplementary Information 4). Considering the habit that young horses are protected by stallion[27], the intensive hunting of young horses may reflect a skilled long-range hunting at the Uluzzian. As the mechanically delivered armatures allow humans more accurate hunting[28] with keeping a long distance from potentially dangerous prey than hand-delivered hunting [but see[29]], this new projectile technology could have offered modern humans an advantage in subsistence strategies.

Methods

Functional analysis

A use-wear analysis was undertaken based on a low-power approach (LPA)[30–33] and a high-power approach (HPA)[34–37]. Out of the 146 backed pieces, 34 pieces were recovered from layer EIII, 60 pieces from layer EII-I, 30 pieces from spit E-D, and 22 pieces from layer D. Traces were observed using a Hirox KH7700 digital microscope at magnifications ranging from 20× to 50× for macro-traces and from 140× to 480× for micro-wear traces.

DIFs were analyzed based on projectile experiments with backed pieces[7,8,38,39]. The DIFs observed on archaeological materials were recorded using the microscope mode of the Olympus TG-4 digital camera. Besides DIFs, 11 backed pieces exhibited possible impact fractures, whereas we cannot rule out the possibility that they formed accidentally due to knapping, retouching, or post-depositional processes[7,39–41]. For instance, pseudo-impact fractures, including tiny flute- and burin-like fractures smaller than 5 mm, can occur throughout production and post-depositional processes. Hence, we did not define these fractures as DIFs.

The use of the bipolar technique on anvil in retouching the Uluzzian backed pieces may create specific pseudo-impact fractures. Therefore, we conducted an experiment on the production of Uluzzian backed pieces to avoid the risk of misidentifying bipolar pseudo-impact scars as “DIFs.” After the careful observation of experimental backed pieces, we confirmed that, although bipolar retouching sometimes produces mimic-DIFs, we can distinguish these from real DIFs based on the presence of a negative bulb of percussion and the position of the fracture initiation (Supplementary Fig. 8).

MLITs are microscopically observable impact scars on lithic surfaces[7,8,42,43]. They comprise clusters of linear polishes running parallel to one another, exhibiting long shining stripes. Although little is currently known about the process of MLIT formation, they probably formed through contact with fragments detached from stone tips or bone of animal targets. Similar linear polish can occur through knapping by a hammer (Supplementary Fig. 8f) and contact with other stone artifacts during transport or storage[37]. However, it is possible to distinguish MLITs from the other linear polishes based on attributes characterized by long, stripe-like linear polishes running in a specific direction with other

linear polishes. The MLITs were recorded using a Hirox microscope at magnifications between 140× and 480×.

Residue analysis

FTIR analyses were performed at the Chemical and Life Sciences branch of the SISSI beamline at Elettra Sincrotrone, Trieste[44].

A total of 10 backed pieces were analyzed by FTIR spectromicroscopy (#100a from layer D, #106 from spit E-D, #75, #1, #34, #64, #45, #52 from layer EII-I, and #21, #23 from layer EIII). A few grains of the adherent residues were gently scraped from each backed piece using the tip of a needle under a stereomicroscope. Collected grains from each sample were pressed within a diamond compression cell (Diamond EX press by S.T. Japan, clear aperture 2 mm) to flatten them to a thickness suitable for FTIR transmission measurements. Due to the heterogeneous nature of the samples, 10–15 spectra for each were acquired in transmission mode on half compression cell with a Vis-IR Bruker Hyperion 3000 microscope coupled with the Vertex 70v interferometer in the MidIR range (MCT-A detector, 4000–750 cm^{-1}). For each spectrum, 512 scans were averaged at 4 cm^{-1} spectral resolution, setting lateral resolution at 50 × 50 μm^2 to select the most diagnostic sample regions accordingly to the observable differences in color.

Spectra of red deposits from layers E and D and soil samples from several stratigraphic units belonging to Grotta del Cavallo (see Supplementary Fig. 1) were also measured by FTIR spectroscopy in the sample compartment of the Vertex 70v interferometer, in the closed diamond compression cell, using a 5X focusing unit (A524/Q, Bruker Optics) and the Bruker wide range components (i.e. beamsplitter and DTGS detector) for covering FIR (Far-Infrared) and MIR (Mid-Infrared) spectral regions in a single scan. Each spectrum was collected averaging 256 scans at 4 cm^{-1}. Indeed, extending the spectral range from 4000 to 150 cm^{-1} allows better highlighting the presence of metal-organic spectral features.

To identify a specific material adhered on lithics, all of the acquired FTIR spectra were compared with that reported in the literature and IR spectral libraries (Kimmel Center for Archaeological Science Infrared Standards Library and IRUG Spectral Database). In addition, samples #1 and #106 were peeled off with carbon conductive adhesive tape from the culet of the diamond after FTIR spectromicroscopy analysis and SEM/EDX measurements were performed. Two red deposits (one from layer D and one from layer EII-I) and a sample of soil from layer DII were also characterized from a mineralogical perspective. All measurements were performed using a Zeiss Supra 40 field emission gun (FEG), SEM equipped with a Gemini column and an in-lens secondary electron detector operated at 10kV. EDX analyses were performed using a LN2-free X-Act Silicon Drift Detector (Oxford X-ray detection system, Aztec EDS). SEM/EDX measurements were performed at the IOM-CNR laboratories (Trieste, Italy).

Among the 10 backed pieces analyzed by FTIR spectromicroscopy, only six (#1, #34, #64, #106, #100a, and #75) showed clear infrared features indicative of an organic fraction (see Fig. 2o). The organic fraction was mainly proven by strong absorption peaks in the range 3000–2800 cm^{-1}, which were assigned to methyl ($-CH_3$) and methylene ($-CH_2$) asymmetric

and symmetric stretching modes at ~2956 and ~2872 cm^{-1}, and ~2930 and ~2860 cm^{-1}, respectively[46]. At ~1460 and ~1378 cm^{-1}, the bending modes of the same moieties can be observed. The aforementioned stretching and bending modes are characteristic of compounds containing long aliphatic chains. In addition, carbonyl (C=O) bands can be detected at around 1740 cm^{-1} for all the selected six samples, and an extra shoulder centered at about 1715 cm^{-1} can be seen for samples #34 #64, #75, and #100a. Typically, carbonyl stretching modes of esters and carboxylic acids fall in this spectral region[47]. Samples #75, #106, and #100a (Fig. 2o) are characterized by two broad bands in the 1650–1550 cm^{-1} and 1450–1350 cm^{-1} spectral regions. The two aforementioned contributions possibly derive from asymmetric and symmetric stretching of COO^- groups usually identified as diagnostic of gum (see the next paragraph for more details)[48]. The aforementioned contributions are less intense for samples #1, #34, and #64 (Fig. 2o), allowing the peak centered at about 1630 cm^{-1} to arise. All the aforementioned spectral ranges are indicated by grey shaded area in Figure 2o.

The collected data led to postulations that the organic fraction is a mixture of two main components: tree or plant gum and beeswax. In particular, the broad peaks in the 1650–1550 and 1450–1350 cm^{-1} spectral regions, can be associated with carboxylate fractions from plant or tree gum, a natural biopolymer comprised mostly of diverse polysaccharides, and, to a much lesser extent, glycoproteins[45,46]. This hypothesis was proven by the spectral comparison of samples #75, #106 and #100a with the reference spectrum of tree gum (Fig. 2o – lower part, brown line), and several other spectra found in the IR databases (see, for example spectra ID ICB00011, ICB00012, ICB00013, and ICB00038 in the IRUG database). Pure and fresh gum spectra are characterized by narrower bands in the aforementioned spectral regions. Nevertheless, it is well known that the peak position of both the asymmetric and symmetric modes of COO^- groups are strongly dependent on the coordinated cations[44]; therefore, band broadening in our samples reflects the complex mineral composition of the soil (see SEM/EDX analysis and Supplementary Fig. 4 for more details). Noteworthy, reference gum spectra show broad unresolved absorption peaks in the range 3000–2800 cm^{-1}, which differ from the signals obtained by measuring our samples that exhibited intense and sharp methyl and methylene stretching modes. This result led to the deduction of the possible addition of a further organic compound to the adhesive, such as beeswax. This hypothesis can be tested by comparison of the collected spectra of samples #1, #34 and #64 with beeswax reference spectra (Fig. 2o – upper part, dark blue line). In the literature, spectra of beeswax (see also ID IWX00075, IWX00090, IWX00096, and IWX00099 in the IRUG database) are characterized by well-defined and intense methyl and methylene bands, as well as by distinctive carbonyl bands centered at about ~1740 and ~1715 cm^{-1}, which were also present in our samples.

Among the collected spectra, it can be observed a variability of the relative intensity of the CH_2/CH_3/C=O bands, mainly characteristic of beeswax (Fig. 2o), with respect to the broad bands extending from about 1650–1550 cm^{-1} and 1450–1350 cm^{-1}, which are characteristic of tree/plant gum (Fig. 2o. This finding can be explained by the different percentages of the two organic fractions used to prepare the adhesive mixture, with additional consideration of the different degree of degradation and aging originating from long-term interaction of the organic material constituting the adhesives with the burial soil[47]. The diverse extent of

degradation of the samples could have been influenced by differences in soil composition, pH, humidity, or water percolation of the stratigraphic units where the 10 backed pieces were buried for thousands of years.

Identification of the gum fraction would have been easier with access to the ~1200–900 cm $^{-1}$ spectral region, where C-O-C and C-OH stretching modes diagnostic of polysaccharides are located[46]. Indeed, in this spectral region, very intense and structured bands can be seen for all 10 measured backed pieces. This feature, characterized by a main peak at 1030 cm^{-1}, a shoulder at 1080 cm^{-1}, and two distinctive peaks at 800 and 780 cm^{-1}, can be attributed to Si-O stretching modes of silicates, which are the main components of clays. Specifically, the sharp peaks at 3694 and 3622 cm^{-1} are distinctive vibrational features of well-crystallized water molecules among the layers of kaolinite[47].

The red color of the residues on the backed pieces led us to hypothesize the presence of iron compounds. To verify this hypothesis, SEM/EDX analyses were performed for a soil sample from layer DII and samples #106 (from spit E-D) and #1 (from layer EII-I) after FTIR analysis (Supplementary Fig. 4b, e, h). EDX of soil and sample #106 confirmed the presence of elements including Si, Al, Mg, Na, Ca, Fe, and P, which are all characteristic of silicates. The iron to silicon ratio increased from 0.37 ± 0.01 to 4.52 ± 2.01 from soil to sample #106, reaching a value of 7.64 ± 0.45 in sample #1 (the standard deviation was calculated as the average of three measurements per sample). The positive trend of the iron to silicon ratio from soil to sample #1 is consistent with a color transition from light brown to intense red (Supplementary Fig. 4a, d, g), revealing that the iron content in the samples is much higher than the one of the burial soil and that it contributes to red pigmentation of the residues on the samples #1 and #106, which can be identified as ochre.

To further verify that ochre (also known as red-earth) is the source of the red color, some red soil deposits that have been collected from Grotta del Cavallo were analyzed by FTIR spectroscopy in the FIR-MIR region. These deposits belong to the same stratigraphic units (layers E and D) of the analyzed backed pieces (see Supplementary Fig. 1). In Supplementary Fig. 5, we report the FIR-MIR spectra of two of the analyzed red deposits. It is possible to identify peaks centered at about 535 and 433 cm^{-1}, as well as a broad band around 325 cm^{-1} that are distinctive of iron oxides. The collected spectra can be correlated with the IRUG ochre spectrum IMP00365 (red earth made by kaolinite and hematite).

Supplementary Fig. 5 also reports the FIR-MIR spectrum of the soil sample from layer DII, also analyzed by SEM/EDX (Supplementary Fig. 4). Notably, this sample does not show the spectral features characteristic of ochre, accordingly with the minimal iron content revealed by SEM/EDX analysis, while it is mainly characterized by a mixture of silicates and phosphates. As a matter of fact, the silicate peaks described above can also be recognized in the FTIR spectrum of the soil, and distinctive features of phosphates can be also identified: two sharp peaks at ~964 and ~870 cm^{-1}, a double peak at ~605 and ~564 cm^{-1} and a moderate absorption band in the 1550 – 1300 cm^{-1} spectral range[49]. The aforementioned phosphate infrared features are still evident in the spectrum of the red deposit from layer D, while they are barely detectable for the red deposit from layer E II-I. This result implies that the red deposit from layer D is partially contaminated by the burial soil while the one from

Europe PMC Funders Author Manuscripts

layer E II-I can be considered as a purer ochre. Notably, none of the spectra reported in Supplementary Fig. 5 show absorbance peaks in the region 3000– 2800 cm^{-1}, which are characteristic of aliphatic chains of organic compounds. This result suggests that, both in the soil and red deposits, the organic matter content is below the detection limit of the technique, thereby excluding the possibility that the organic traces on backed pieces are contamination from the burial environment.

Taken together, these results led us to conclude that the residue stuck on the backed pieces is a mixture of plant/tree gum and beeswax intentionally mixed with ochre and applied as an adhesive.

Morphometric analysis

As the Uluzzian backed pieces are extremely small (Supplementary Figs. 6a, 7b), they are not suitable to haft onto the tip of thick wooden spears from Schöningen in Germany dated ~300 ka[50–52], which were likely used as throwing spears[53,54] (Supplementary Fig. 7a). It has been ethnographically shown that thrusting spears and hand-delivered spears are heavier than projectile spears launched with a spearthrower or bow[55,56]. Therefore, the Uluzzian backed pieces do not function well as throwing or thrusting spear tips, which require a massive shaft. If the Uluzzian backed pieces were inserted into the lateral sides of a shaft as Magdalenian composite projectiles[57], the smallness of the stone artifacts would not necessarily relate to the diameter of the shaft. However, as the use-wear analysis suggested that a considerable number of Uluzzian pieces were attached to the tip of a shaft as a hunting armature, the small dimensions must reflect a thin shaft that is useful for only mechanically delivered spears, such as darts projected by a spearthrower or arrows shot using a bow.

Hence, a morphometric analysis using TCSA and TCSP values was undertaken to evaluate the potential projectile capability of stone tips[20,56,58,59]. TCSA and TCSP values of Uluzzian backed pieces from Grotta del Cavallo were compared to those of ethnographic North American dart tips and arrowheads[12,13]. Because some Uluzzian backed pieces were used for cutting and scraping, the TCSA and TCSP analyses were undertaken only for the backed pieces showing DIFs (Supplementary Fig. 6b, c). The TCSA and TCSP values were calculated using the equations presented by Sisk & Shea[59].

Supplementary Material

Refer to Web version on PubMed Central for supplementary material.

Acknowledgements

We thank Soprintendenza Archeologia, Belle Arti e Paesaggio per le Province di Brindisi, Lecce e Taranto, and especially Drs. Maria Piccarreta and Serena Strafella for kindly supporting our research at Grotta del Cavallo. Special thanks are due to Professors Arturo Palma di Cesnola and Paolo Gambassini for giving us the opportunity to revisit the Uluzzian materials from their excavations. We are grateful to Professor Lucia Sarti for providing the base planimetry of Grotta del Cavallo. We also acknowledge Elettra Sincrotrone Trieste for provision of synchrotron radiation facilities (proposal No. 20180262) and Weizmann Institute of Science for providing the Kimmel Center for Archaeological Science Infrared Standards Library. Finally, we thank Professor Ilaria Corsi for providing contacts between the University of Siena and Elettra Sincrotrone Trieste. This research was supported by a grant from the European Research Council (ERC-724046, SUCCESS; http://www.erc-success.eu/). K.S. was supported by MEXT/JSPS KAKENHI grant numbers JP17H06381 in #4903 and 15H05384.

References

1. Moroni A, et al. Grotta del Cavallo (Apulia-Southern Italy). The Uluzzian in the mirror. J Anthropol Sci. 2018; 96:125–160. [PubMed: 30036183]
2. Zanchetta G, Giaccio B, Bini M, Sarti L. Tephrostratigraphy of Grotta del Cavallo, Southern Italy: insights on the chronology of Middle to Upper Palaeolithic transition in the Mediterranean. Quaternary Science Reviews. 2018; 182:65–77.
3. Giaccio B, Hajdas I, Isaia R, Deino A, Nomade S. High-precision 14C and 40Ar/39Ar dating of the Campanian Ignimbrite (Y-5) reconciles the time-scales of climatic-cultural processes at 40 ka. Sci Rep. 2017; 7:1–10. [PubMed: 28127051]
4. d'Errico F, Borgia V, Ronchitelli A. Uluzzian bone technology and its implications for the origin of behavioural modernity. Quaternary International. 2012; 259:59–71.
5. Moroni A, Boscato P, Ronchitelli A. What roots for the Uluzzian? Modern behaviour in Central-Southern Italy and hypotheses on AMH dispersal routes. Quaternary International. 2013; 316:27–44.
6. Palma di Cesnola A. Il Paleolitico superiore arcaico (Facies uluzziana) della Grotta del Cavallo (Continuazione), Lecce. Rivista Scienze Preistoriche. 1966; 21:3–59.
7. Fischer A, Hansen PV, Rasmussen P. Macro- and microwear traces on lithic projectile points. Experimental results and prehistoric examples. Journal of Danish Archaeology. 1984; 3:19–46.
8. Sano K, Oba M. Backed point experiments for identifying mechanically-delivered armatures. Journal of Archaeological Science. 2015; 63:13–23.
9. Bradtmöller M, Sarmiento A, Perales U, Zuluaga MC. Investigation of Upper Palaeolithic adhesive residues from Cueva Morín, Northern Spain. Journal of Archaeological Science: Reports. 2016; 7:1–13.
10. Yaroshevich A, Kaufman D, Nuzhnyy D, Bar-Yosef O, Weinstein-Evron M. Design and performance of microlith implemented projectiles during the Middle and the Late Epipaleolithic of the Levant: experimental and archaeological evidence. Journal of Archaeological Science. 2010; 37:368–388.
11. Goldstein ST, Shaffer CM. Experimental and archaeological investigations of backed microlith function among Mid-to-Late Holocene herders in southwestern Kenya. Archaeol Anthropol Sci. 2017; 9:1767–1788.
12. Thomas DH. Arrowheads and atlatl darts: how the stones got the shaft. American Antiquity. 1978; 43:461–472.
13. Shott MJ. Stones and shafts redux: the metric discrimination of chipped-stone dart and arrow points. American Antiquity. 1997; 62:86–101.
14. Wadley L. Putting ochre to the test: replication studies of adhesives that may have been used for hafting tools in the Middle Stone Age. Journal of Human Evolution. 2005; 49:587–601. [PubMed: 16126249]
15. Cattelain P. Un crochet de propulseur solutréen de la grotte de Combe-Saunière 1 (Dordogne). Bulletin de la Société préhistorique française. 1989; 86:213–216.
16. Rust, A. Die alt- und mittelsteinzeitlichen Funde von Stellmoor. Karl Wachholtz Verlag; 1943.
17. Stodiek, U. Zur Technologie der jungpaläolithischen Speerschleuder: eine Studie auf der Basis archäologischer, ethnologischer und experimenteller Erkenntnis. Verlag Archaeologica Venatoria, Institut für Ur- und Frühgeschichte der Universität Tübingen; 1993.
18. Thieme H, Veil S. Neue Untersuchungen zum eemzeitlichen Elefanten-Jagdplatz Lehringen, Ldkr. Verden. Die Kunde. 1985; 36:11–58.
19. Villa P, Boscato P, Ranaldo F, Ronchitelli A. Stone tools for the hunt: points with impact scars from a Middle Paleolithic site in southern Italy. Journal of Archaeological Science. 2009; 36:850–859.
20. Shea JJ. The origins of lithic projectile point technology: evidence from Africa, the Levant, and Europe. Journal of Archaeological Science. 2006; 33:823–846.
21. Metz, L. Le troisième Homme Préhistoire de lAltaï. Musée national de la Préhistoire; 2017. 156–160.

Europe PMC Funders Author Manuscripts

22. Slimak L. For a cultural anthropology of the last Neanderthals. Quaternary Science Reviews. 2019; 217:330–339.
23. Villa P, Soriano S. Hunting weapons of Neanderthals and early modern humans in South Africa: similarities and differences. Journal of Anthropological Research. 2010; 66:5–38.
24. Wadley L, Mohapi M. A Segment is not a Monolith: evidence from the Howiesons Poort of Sibudu, South Africa. Journal of Archaeological Science. 2008; 35:2594–2605.
25. Zilhão J, Banks WE, d'Errico F, Gioia P. Analysis of site formation and assemblage integrity does not support attribution of the Uluzzian to Modern Humans at Grotta del Cavallo. PLoS ONE. 2015; 10:131–181.
26. Benazzi S, et al. Early dispersal of modern humans in Europe and implications for Neanderthal behaviour. Nature. 2011; 479:525–528. [PubMed: 22048311]
27. Heptner, VG, Nasimovich, AA, Bannikov, AG. Mammals of the Soviet Union, Volume I, Artiodactyla and Perissodactyla. Smithsonian institution Libraries and the National Science Foundation; 1988.
28. Lew-Levy S, Reckin R, Lavi N, Cristóbal-Azkarate J, Ellis-Davies K. How do hunter-gatherer children learn subsistence skills? Hum Nat. 2017; 28:367–394. [PubMed: 28994008]
29. Milks A, Parker D, Pope M. External ballistics of Pleistocene hand-thrown spears: experimental performance data and implications for human evolution. Sci Rep. 2019; 9
30. Tringham R, Cooper G, Odell G, Voytek B, Whitman A. Experimentation in the formation of edge damage: a new approach to lithic analysis. Journal of Field Archaeology. 1974; 1:171–196.
31. Odell GH, Odell-Vereecken F. Verifying the reliability of lithic use-wear assessments by 'blind tests': the Low-Power Approach. Journal of Field Archaeology. 1980; 7:87–120.
32. Odell GH. The mechanics of use-breakage of stone tools: some testable hypotheses. Journal of Field Archaeology. 1981; 8:197–209.
33. Akoshima, K. In: Sieveking, GD; Newcomer, MH, editors. The Human Uses of Flint and Chert. Proceedings of the fourth international flint symposium held at Brighton Polytechnic; 10-1 April 1983; Cambridge University Press; 1987. 71–79.
34. Keeley, LH. Experimental Determination of Stone Tool Uses: A Microwear Analysis. University of Chicago Press; 1980.
35. Vaughan, PC. Use-Wear Analysis of Flaked Stone Tools. The University of Arizona Press; 1985.
36. Van Gijn, AL. The Wear and Tear of Flint: Principles of Functional Analysis Applied to Dutch Neolithic Assemblages. University of Leiden; 1990.
37. Sano, K. Functional Variability in the Late Upper Palaeolithic of North-Western Europe. Rudolf Habelt Verlag; 2012.
38. Lombard M. Finding resolution for the Howiesons Poort through the microscope: micro-residue analysis of segments from Sibudu Cave, South Africa. Journal of Archaeological Science. 2008; 35:26–41.
39. Pargeter J. Rock type variability and impact fracture formation: working towards a more robust macrofracture method. Journal of Archaeological Science. 2014; 40:4056–4065.
40. Sano K. Hunting evidence from stone artefacts from the Magdalenian cave site Bois Laiterie, Belgium: a fracture analysis. Quartär. 2009; 56:67–86.
41. Pargeter J. Assessing the macrofracture method for identifying Stone Age hunting weaponry. Journal of Archaeological Science. 2011; 38:2882–2888.
42. Moss EH, Newcomer MH. Reconstruction of tool use at Pincevent: microwear and experiments. Studia Praehistorica Belgica. 1982; 2:289–312.
43. Geneste, JM, Plisson, H. Before Lascaux: The Complex Record of the Early Upper Paleolithic. Knecht, H, Pike-Tay, A, White, R, editors. CRC Press; 1993. 117–135.
44. Lupi S, et al. Performance of SISSI, the infrared beamline of the ELETTRA storage ring. J Opt Soc Am B, JOSAB. 2007; 24:959–964.
45. Espinosa-Andrews H, Sandoval-Castilla O, Vazquez-Torres H, Vernon-Carter EJ, Lobato-Calleros C. Determination of the gum Arabic–chitosan interactions by Fourier Transform Infrared Spectroscopy and characterization of the microstructure and rheological features of their coacervates. Carbohydrate Polymers. 2010; 79:541–546.

46. Petrea P, Amarioarei G, Apostolescu N, Puitel AC, Ciovica S. Some aspects of the characterization of vegetable gums: *Prunus persica* (plum) and *prunus domestica* (cherry). Cellulose Chemistry and Technology. 2013; 47:369–375.
47. Socrates, G. Infrared and Raman Characteristic Group Frequencies Tables and Charts. Socrates, G, editor. Wiley; 2001. 283–340.
48. van der Marel HW, Krohmer P. O-H stretching vibrations in kaolinite, and related minerals. Contr Mineral and Petrol. 1969; 22:73–82.
49. Fleet ME. Infrared spectra of carbonate apatites: ν2-Region bands. Biomaterials. 2009; 30:1473–1481. [PubMed: 19111895]
50. Sierralta, M, Frechen, M, Urban, B. Die chronologische Einordnung der paläolithischen Fundstellen von Shöningen. Forschungen zur Urgeschichte aus dem Tagebau von Schöningen Band 1. Behre, K-E, editor. Verlag des Römisch-Germanischen Zentralmuseums; 2012. 143–154.
51. Urban, B, Sierralta, M. Die chronologische Einordnung der paläolithischen Fundstellen von Shöningen. Forschungen zur Urgeschichte aus dem Tagebau von Schöningen. Behre, K-E, editor. Vol. 1. Verlag des Römisch-Germanischen Zentralmuseums; 2012. 77–96.
52. Richter D, Krbetschek M. The age of the Lower Paleolithic occupation at Schöningen. Journal of Human Evolution. 2015; 89:46–56. [PubMed: 26212768]
53. Thieme H. Lower Palaeolithic hunting spears from Germany. Nature. 1997; 385:807–810. [PubMed: 9039910]
54. Thieme, H. The Hominid Individual in Context: Archaeological investigations of Lower and Middle Palaeolithic landscapes, locales and artefacts. Gamble, C, Porr, M, editors. Routledge; 2005. 115–132.
55. Cattelain, P. Projectile Technology. Knecht, H, editor. Plenum Press; 1997. 213–240.
56. Hughes SS. Getting to the point: evolutionary change in prehistoric weaponry. Journal of Archaeological Method and Theory. 1998; 5:345–408.
57. Pétillon J-M, et al. Hard core and cutting edge: experimental manufacture and use of Magdalenian composite projectile tips. Journal of Archaeological Science. 2011; 38:1266–1283.
58. Shea JJ, Sisk ML. Complex projectile technology and *Homo sapiens* dispersal into western Eurasia. PaleoAnthropology. 2010; 2010:100–122.
59. Sisk ML, Shea JJ. The African origin of complex projectile technology: an analysis using tip cross-sectional area and perimeter. International Journal of Evolutionary Biology. 2011; 2011:1–8.
60. Waelbroeck C, et al. Sea-level and deep water temperature changes derived from benthic foraminifera isotopic records. Quaternary Science Reviews. 2002; 21:295–305.

Europe PMC Funders Author Manuscripts

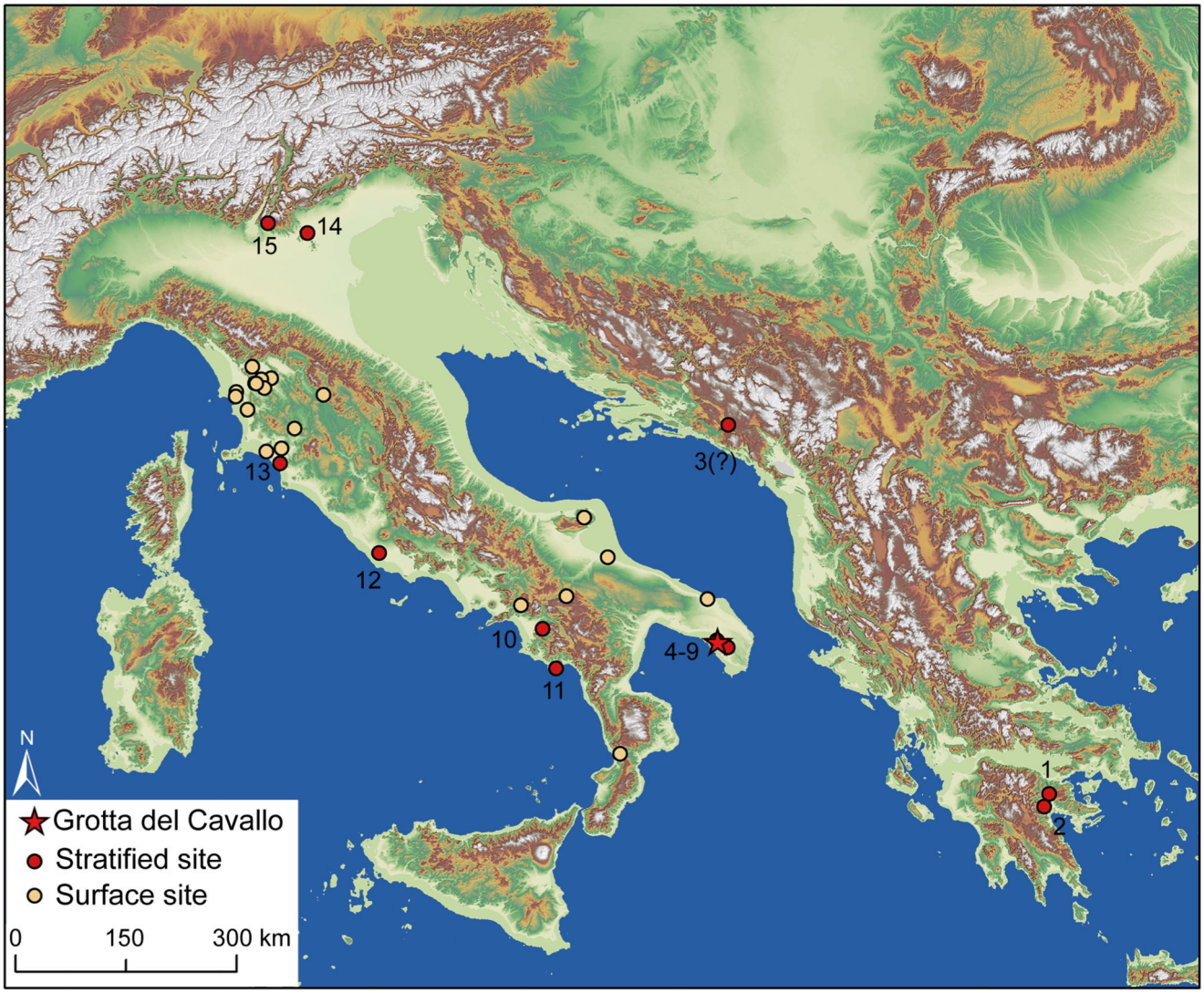

Fig. 1. Locations of the Uluzzian findings in Italy and on the Balkan Peninsula.

(1) Klissoura Cave, (2) Kephalari Cave, (3) Crvena Stijena, (4) Grotta del Cavallo, (5) Grotta di Serra Cicora A, (6) Grotta Mario Bernardini, (7) Grotta di Uluzzo, (8) Grotta di Uluzzo C/Cosma, (9) Grotta delle Veneri, (10) Grotta di Castelcivita, (11) Grotta della Cala, (12) Colle Rotondo, (13) Grotta La Fabbrica, (14) Riparo del Broion, (15) Grotta di Fumane. Sea level 74 m below the present-day coastline (ref. 60). Source of digital elevation model: European DEM from the GMES RDA project (https://www.eea.europa.eu/data-and-maps/data/eu-dem#tab-original data/eudem_hlsd_3035_europe). Source of bathymetric model: European Marine Observation and Data Network (EMODnet). The map was generated using ArcGIS® 10.5.

Europe PMC Funders Author Manuscripts

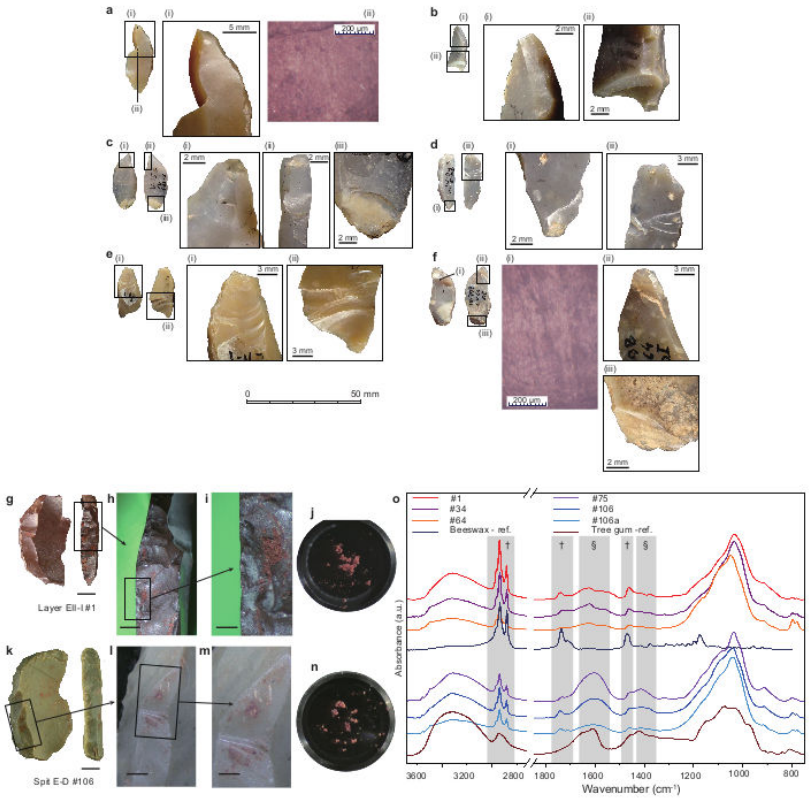

Fig. 2. Backed pieces from Grotta del Cavallo showing DIFs and MLITs, and sampling of residues on backed pieces by FTIR spectroscopy and its results.

a, A simple DIF type a2. **b**–**f**, Multiple DIF type a2m. a(i), c(ii) and d(i) are burin-like fractures; b(i), c(i), and c(iii) are flute-like fractures; b(ii) is a step-terminating transverse fracture and a spin-off; e(i) and d(ii) are spin-offs; e(ii) is a step-terminating transverse fracture; f(ii) is flute- and burin-like fractures; f(iii) is a feather-terminating transverse fracture. a(ii), f(i) and the black lines in **a** and **f** are MLITs. **b**, **c** and **e** are from layer EII-I; **a** and **d** are from layer E-D; and **f** is from layer D. **g**, **k**, Optical images at two different angles

of sample 1, layer EII-I (scale bar, 5 mm) and sample 106, spit E-D (scale bar, 5 mm). Sampled areas are highlighted by a black box and magnified in **h** and **i** for sample 1 (scale bars, 1 mm and 0.5 mm) and in **l**, and **m** for sample 106 (scale bars, 2 mm and 1 mm). **j**, **n** Optical images of the scraped residues sitting on the culet of the opened diamond compression cell. **o**, Representative FTIR spectra of the sampled residues from samples 1, 34, 64, 75, 106 and sample 100a. Two selected reference spectra of beeswax and peach tree gum are also plotted using the database from Kimmel Center for Archaeological Science Infrared Standards Library (https://www.weizmann.ac.il/kimmel-arch/infrared-spectra-library). The grey shaded areas indicate the main absorption bands, characteristic of the organic fraction. Among them, those relating to beeswax are marked with dagger symbols, and those relating to plant/tree gum are marked with section symbols. For more details on the band positions and assignments, refer to the Methods.

Europe PMC Funders Author Manuscripts